

Feasibility of using the threshold photoemission in studies of surface states of submonolayer metal films

G. V. Benemanskaya, M. N. Lapushkin, and M. I. Urbakh

A. F. Ioffe Physicotechnical Institute, Russian Academy of Sciences

(Submitted 22 May 1992)

Zh. Eksp. Teor. Fiz. **102**, 1664–1673 (November 1992)

A proposed theory of threshold photoemission allows for the existence of a local surface band with the binding energy close to the Fermi level. An expression is obtained for a matrix element corresponding to surface photoexcitation and a study is made of the dependence of this element on the parameters of the local energy band. The bulk (volume) and surface photoemission currents are calculated. It is shown that the frequency, angular, and polarization dependences of the threshold photoemission can be used to determine the fundamental parameters of the photoelectron states of the surface and of adsorbed submonolayer coatings. The anomalously large contribution of the surface to the threshold photoemission is explained. Calculations and an analysis of the experimental data for the W(110)–Cs system are reported. The main characteristics of the surface electron energy band induced by Cs coating are determined for the first time.

1. INTRODUCTION

A submonolayer coating can be regarded as the initial stage of the formation of an interface when the coating initiates the greatest changes in the electron structure of the substrate and gives rise to new electron states on the surface and at the interface. In the case of a metal substrate and a metal coating all the changes in the electron structure caused by the adsorption of atoms on the surface are localized in a narrow layer (representing one or two lattice constants) because of the strong screening.¹ It follows that the methods for the investigation of the electron structure of the surface should be designed to apply either to a small depth of a data-carrying response or to a small depth of the excitation. Current investigations of the surface states of metals are being made exclusively by the methods of photoelectron spectroscopy using high-energy synchrotron, x-ray, or ultraviolet radiation and utilizing the minimal depth of photoelectron emission at such energies. This approach has been employed to detect the intrinsic surface states located near the Fermi level E_F for different single-crystal faces of metals such as W (Refs. 2 and 3), Al (Ref. 4), Cu, Ag, and Au (Ref. 5).

However, the traditional investigations have proved much less effective in the search for and the study of the surface states induced by a submonolayer coating characterized by $\theta_a \ll 1$ (where the surface coverage corresponding to a monolayer is $\theta_a = 1$). The most informative are the experiments carried out for the W(100)–Cs system using p -polarized synchrotron radiation.³ The initial photoemission spectrum reveals clearly a peak of the intrinsic surface states of W(100) with an energy 0.3 eV below E_F . The process of deposition of a submonolayer Cs coating shifts the peak of the surface states linearly toward higher binding energies and stabilizes its position (at $E = 1.3$ eV) when the coverage reaches $\theta_a = 0.6$. The spectrum shows no evidence of new surface states associated with the deposition of the Cs coating. The W(110)–Cs system had been investigated also⁶ by excitation with p -polarized light of frequencies close to the photoemission threshold. The results revealed the surface

photoemission from new states which appear when $\theta_a \gtrsim 0.6$.

There have been several investigations that have revealed induced surface states manifested in the photoemission spectra of the following systems: Cu(111)–Cs (Ref. 7), Cu(111)–Na (Ref. 8), W(110)–Ba (Ref. 9), W(110)–Cs, W(100)–Cs (Ref. 6), Al(111)–K (Refs. 10 and 11), and W(111)–Cs (Ref. 12). All these investigations have been concerned with submonolayer coatings consisting of alkali or alkaline-earth metal atoms. These coatings are characterized by a high polarizability, a considerable redistribution of the electron density in the region of the metal–adatom bonds, and a considerable influence of the coating on the work function.¹ When atoms are adsorbed singly, the local valence states of an adatom become strongly perturbed and this is manifested by a shift and broadening of these levels.

An increase in the thickness of the submonolayer coating results in a direct overlap of the wave functions of adatoms and formation of induced two-dimensional surface states. Experiments show that such states have a negligible binding energy. One feature of these investigations should be mentioned, namely the use of excitations of relatively low energies. In the investigations reported in Refs. 6 and 9 the induced surface states were revealed by p -polarized excitation from the optical range and involved an investigation of the dependences of the threshold photoemission on the various characteristics of the system and radiation. These results conflict somewhat with the current ideas on the nature of the threshold photoemission postulating a considerable depth of excitation and emission of photoelectrons. Therefore, the possibility of obtaining information on the surface states has not been considered so far in theoretical investigations of the threshold photoemission.

We shall develop a theory of the threshold photoemission in the presence of a local electron state on the surface of a metal and we shall assume that the energy of this state is of the order of the Fermi level. We shall obtain an expression for a matrix element describing a photoemission transition, study the influence of various parameters of the surface states, and calculate the threshold photoemission spectrum

for p -polarized excitation. We shall then use the results in an analysis of the experimental threshold photoemission spectra of the W(110)-Cs system. We shall show that the set of the spectral and angular photoemission characteristics carries information on such fundamental parameters of the surface states as the position of the energy band and its half-width, and the value of the matrix element.

2. MODEL AND PRINCIPAL RELATIONSHIPS

We shall assume that at an interface between vacuum and a metal with a bulk permittivity $\epsilon_m(\omega) = \epsilon'_m(\omega) + i\epsilon''_m(\omega)$ there is a two-dimensional electron energy band with a local density of states $\rho_a(E)$, with its maximum at E_0 relative to the vacuum level, and with a half-width 2Γ (Fig. 1a). We shall assume that the coordinate x_1 is directed along the normal to the surface, whereas the coordinates x_2 and x_3 are parallel to the surface, and that the plane of incidence of light coincides with the x_1x_2 plane. When polarized light is incident on a surface at an angle γ , the components of the electric field parallel to the surface change slowly along the surface and they can be regarded as constant over a distance equal to the wavelength of light:

$$\begin{aligned} \mathcal{E}_2 &= -[1+r_p(\gamma, \omega)] \mathcal{E}_p \cos \gamma, \\ \mathcal{E}_3 &= [1-r_s(\gamma, \omega)] \mathcal{E}_s, \end{aligned} \quad (1)$$

where \mathcal{E}_p and \mathcal{E}_s are the amplitudes of the p - and s -polarized light waves incident on the surface; r_p and r_s are the amplitudes of the reflection coefficients of the incident light. We shall assume in future that $\mathcal{E}_p = \mathcal{E}_s = \mathcal{E}_0$.

However, the normal component of the electric field varies near the surface^{13,14} and can be described approximately by the expression

$$\mathcal{E}_1(x_1) = \frac{1}{\epsilon_{\text{eff}}(x_1)} [1-r_p(\gamma, \omega)] \mathcal{E}_0 \sin \gamma, \quad (2)$$

where ϵ_{eff} is the effective permittivity which at atomic distances $2d$ (amounting to several angstroms) changes from the bulk permittivity $\epsilon_m(\omega)$ to the permittivity of vacuum $\epsilon = 1$ (Fig. 1b). In the photoemission process it is important that in the optical frequency range we have $|\epsilon_m| \gg 1$. Therefore, the field $\mathcal{E}_1(x_1)$ acting directly at the surface, where there is a local energy band characterized by ρ_a , is much (by a factor $|\epsilon_m|$) greater than the field in the bulk of the metal. We can also point out that in the optical frequency range we have $|1+r_p| \ll |1-r_p|$ and—as demonstrated by Eqs. (1) and (2)—directly at the surface the normal component of the field is much greater than the parallel components. It follows that, even though the thickness of the region from which bulk photoemission takes place is much greater than the thickness of the adsorbed layer, in the optical frequency range the adsorbate can make the dominant contribution to the photoemission process.

Simultaneous measurements of the frequency and polarization dependences of the photoemission parameters can, in principle, provide important information on the photoexcitation mechanism, as well as on the electronic characteristics of the surface and of the layers adsorbed on it. This information can be obtained from the experimental data only if we have a theory that relates the observed threshold photoemission signals to the microscopic structure of the surface.

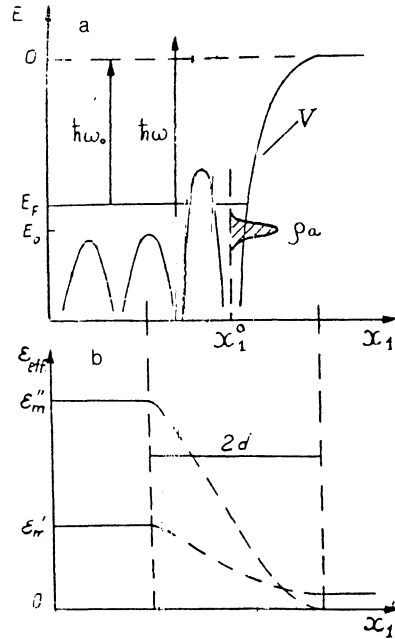


FIG. 1. a) Coulomb potential $V(x_1)$, where x_1 is the normal to the surface, x_1^0 is the position of the adsorbed atoms, $\rho(E)$ is the local density of the surface states, and E_0 is the energy position of the maximum. b) Schematic representation of the changes in the effective permittivity $\epsilon_{\text{eff}}(x_1)$ at a metal-vacuum interface.

A matrix element M_j of an optical transition determines the value of the photocurrent and can be written as follows:

$$\begin{aligned} M_j &\propto \int dx \Psi_f(\mathbf{x}, E_i + \hbar\omega, \mathbf{p}_{\parallel}) \\ &\times \left[\frac{\partial}{\partial x_j} \mathcal{E}_j(\mathbf{x}) + \mathcal{E}_j(\mathbf{x}) \frac{\partial}{\partial x_j} \right] \Psi_i^*(\mathbf{x}, E_i, \mathbf{p}_{\parallel}). \end{aligned} \quad (3)$$

Here, $\Psi_i(\mathbf{x}, E_i, \mathbf{p}_{\parallel})$ and $\Psi_f(\mathbf{x}, E_i + \hbar\omega, \mathbf{p}_{\parallel})$ are the normalized wave functions of the initial (i) and final (f) states with the energies E_i and $E_i + \hbar\omega$ and with the projections of the quasimomenta p_{\parallel} along the surface plane; $\mathcal{E}_j(\mathbf{x})$ is the component of the electric field which induces the investigated phototransition. The energy is measured from the vacuum level $E_{\text{vac}} = 0$.

In describing the photoemission in the threshold frequency range we shall use the following generally accepted expression for the density of the photoemission current:^{13,15}

$$I \propto \int dE_i \int d^2 p_{\parallel} |M_j|^2 \theta(E_F - E_i) \theta(E_i + \hbar\omega - \frac{p_{\parallel}^2 \hbar^2}{2m}). \quad (4)$$

The integration is carried out in Eq. (4) over all the occupied initial states with the energy E_i ($E_i < E_F$) and the function $\theta(E_i + \hbar\omega - p_{\parallel}^2 \hbar^2 / 2m)$ allows for the fact that the contribution to the current comes only from those electrons whose energy of motion along the normal to the surface obeys the inequality $(E_i + \hbar\omega - p_{\parallel}^2 \hbar^2 / 2m) > 0$.

The optical transitions responsible for photoemission may occur, firstly, due to the potentials of the ionic cores in that part of the interior of the solid substrate where the electromagnetic field ($\mathcal{E}_2, \mathcal{E}_3$) represents an already established field of the refracted wave (bulk photoeffect) and, secondly, directly near the surface which can be clean or may carry an adsorbed layer, due to the action of the normal component of

the electric field \mathcal{E}_1 , depending on the coordinate x_1 [see Eq. (2)].

In the threshold frequency range the bulk component of the photocurrent for the s - and p -polarized light can be written in the form:¹³

$$I_s = |K|^2 (\omega - \omega_0)^2 \theta(\omega - \omega_0) \frac{\mathcal{E}_0^2 |M_3^b|^2 \cos \gamma}{|\cos \gamma + (\epsilon_m - \sin^2 \gamma)^{1/2}|^2}, \quad (5)$$

$$I_p = |K|^2 (\omega - \omega_0)^2 \theta(\omega - \omega_0) \frac{\mathcal{E}_0^2 \cos \gamma}{|\epsilon_m \cos \gamma + (\epsilon_m - \sin^2 \gamma)^{1/2}|^2} \times \{ |M_2^b|^2 |\epsilon_m - \sin^2 \gamma| + |M_1^b|^2 |\epsilon_m|^2 \sin^2 \gamma + \text{Re}[(M_1^b)^* \epsilon_m^* M_2^b (\epsilon_m - \sin^2 \gamma)^{1/2}] \sin \gamma \}, \quad (6)$$

where ω_0 is the threshold frequency; K is a constant which includes factors independent of ω in the threshold approximation and governing the behavior of the density of states near the Fermi surface as well as the properties of the transmission coefficient (transparency) of the surface barrier; M_i^b ($i = 1, 2, 3$) are the matrix elements of the transitions involving the ionic cores and induced by the i th component of the electric field \mathcal{E}_i . The factor $(\omega - \omega_0)^2 \theta(\omega - \omega_0)$ is a consequence of integration over the phase volume, permitted by the laws of conservation.

In the case of s -polarized light, for which the component of the electric field \mathcal{E}_3 [see Eq. (1)] hardly changes near the surface, we can ignore the influence of an adsorbed submonolayer coating on the photoemission current, because the effective thickness of this layer is much less than the thickness of the surface metal layer that contributes to the bulk photocurrent (the latter is of the order of the mean free path, which is $\sim 100 \text{ \AA}$).

In the case of p -polarized light we have to consider separately the effects of the normal and tangential components of the electric field. The influence of the tangential component of the field gives rise to a process of bulk photoemission similar to that induced by s -polarized light. The situation changes qualitatively in the case of the photoemission process when the normal component of the electric field \mathcal{E}_1 is excited and which changes rapidly near the surface. According to Eq. (2) the field in the part of the metal substrate contributing to the bulk photoeffect is much less than directly near the surface. Therefore, even in spite of the small thickness of the adsorption layer, the surface photoemission may be stronger than the bulk effect. It should be mentioned also that optical transitions involving a surface potential barrier can also increase the surface photocurrent. These processes may result in a situation that the influence of the surface and adsorbed layer may become dominant. The total photocurrent due to the excitation with p -polarized light obtained allowing for the bulk current and for the surface photoemission can be described as follows:

$$I_p = |K|^2 \theta(\omega - \omega_0) \frac{\mathcal{E}_0^2 \cos \gamma}{|\epsilon_m \cos \gamma + (\epsilon_m - \sin^2 \gamma)^{1/2}|^2} \times \{ |M_2^b|^2 (\omega - \omega_0)^2 |\epsilon_m - \sin^2 \gamma| + |M_1^b|^2 |\epsilon_m|^2 \sin^2 \gamma + 2(\omega - \omega_0) \text{Re}[(M_1^b)^* \epsilon_m^* M_2^b (\epsilon_m - \sin^2 \gamma)^{1/2}] \sin \gamma \}, \quad (7)$$

where the matrix element M_1 includes the bulk M_1^b and surface M_1^s matrix elements:

$$M_1 = M_1^s + M_1^b (\omega - \omega_0). \quad (8)$$

3. PHOTOEMISSION FROM SURFACE STATES

The surface photoemission current induced by the normal component \mathcal{E}_1 of p -polarized light can be described as follows:^{13,16}

$$I_{\text{surf}} \propto \int dE_i \int d^2 p_{\parallel} \theta(E_F - E_i) \theta\left(E_i + \hbar\omega - \frac{p_{\parallel}^2 \hbar^2}{2m}\right) \times \left[\int_L d^3 x \Psi_i(x, E_i + \hbar\omega, \mathbf{p}_{\parallel}) \left[\frac{1}{\epsilon_{\text{eff}}(x_1)} \frac{\partial}{\partial x_1} + \frac{1}{2} \frac{\partial}{\partial x_1} \frac{1}{\epsilon_{\text{eff}}(x_1)} \right] \times \Psi_i^*(x, E_i, \mathbf{p}_{\parallel}) \right]^2 \mathcal{E}_0^2 |1 - r_p(\gamma, \omega)|^2 \frac{\sin^2 \gamma}{\cos \gamma} \approx \int dE_i \int d^2 p_{\parallel} \theta(E_F - E_i) \theta\left(E_i + \hbar\omega - \frac{p_{\parallel}^2 \hbar^2}{2m}\right) \times \left[\int_L d^3 x \Psi_i(x, E_i + \hbar\omega, \mathbf{p}_{\parallel}) \frac{\partial}{\partial x_1} \Psi_i(x, E_i, \mathbf{p}_{\parallel}) \right]^2 \times \left| \frac{1}{\epsilon_{\text{eff}}(x_1^0)} \right|^2 \frac{\mathcal{E}_0^2 |\epsilon_m|^2 \cos \gamma \sin^2 \gamma}{|\epsilon_m \cos \gamma + (\epsilon_m - \sin^2 \gamma)^{1/2}|^2}. \quad (9)$$

Integration in Eq. (9) is carried out over a surface region L and x_1^0 represents the positions of the centers of the adsorbed atoms. In writing down the second part of Eq. (9) it is assumed that the width or thickness of the region $2d$ where the permittivity $\epsilon_{\text{eff}}(x_1)$ changes exceeds the characteristic size of the region of change in the surface potential. Usually this condition is satisfied.¹⁶

In the calculation of the matrix element occurring in Eq. (9) we shall assume that the main contribution to the photoemission process is made by the optical transitions from electron states on the surface, which are characterized by the following local density distribution:

$$\rho_a(E) = \frac{1}{\pi} \frac{\theta_a \Gamma}{(E - E_0)^2 - \Gamma^2}. \quad (10)$$

The wave function of the initial state can be represented in the form

$$\Psi_i(x, E_i, \mathbf{p}_{\parallel}) = \Psi_m(x, E_i, \mathbf{p}_{\parallel}) + \sum_{\mathbf{x}_2^0, \mathbf{x}_3^0} \int d^2 p_{\parallel}' T_a(\mathbf{p}_{\parallel}, \mathbf{p}_{\parallel}', E_i) \Phi_a(x, E_0), \quad (11)$$

where Ψ_m is the wave function of the metal free of the adsorbate; Φ_a is a wave function corresponding to the investigated electron states of the adsorbed atoms; $T_a(p_{\parallel}, p_{\parallel}', E_i)$ is the scattering matrix. The summation in Eq. (11) is carried out over the positions of the atoms along the surface. According to the results of the calculations carried out, for example, using the Anderson model,¹⁷ the matrix T_a has a pole at $E = E_0 + i\Gamma$:

$$T_a = \frac{a(p_{\parallel}) a(p_{\parallel}')}{E - E_0 - i\Gamma} + \dots, \quad (12)$$

where $a(p_{\parallel})$ is the scattering form factor.

Substituting Eqs. (10) and (11) into Eq. (9), we obtain the following expression for the surface photocurrent associated with the excitation of the surface states:

$$I_{\text{surf}} = |K|^2 \frac{\theta_a}{|\epsilon_{\text{eff}}(x_1^0)|^2} \frac{\mathcal{E}_0^2 |\epsilon_m|^2 \cos \gamma \sin^2 \gamma}{|\epsilon_m \cos \gamma + (\epsilon_m - \sin^2 \gamma)^{1/2}|^2} \times \Gamma \left\{ \frac{E_0 - \hbar\omega}{\Gamma} \left[\arctan\left(-\frac{E_0 + \hbar\omega_0}{\Gamma}\right) - \arctan\left(-\frac{E_0 + \hbar\omega}{\Gamma}\right) \right] \right\}$$

$$+ \frac{1}{2} \ln \left| \frac{(E_0 + \hbar\omega_0)^2 + \Gamma^2}{(E_0 + \hbar\omega)^2 + \Gamma^2} \right| \Bigg\} \\ \times \left| \int_L d^3x \Psi_f(x, E, +\hbar\omega, 0) \frac{\partial}{\partial x_1} \Phi_a(x, E_0) \right|^2. \quad (13)$$

The frequency dependence of the last factor in Eq. (13) can be approximated by a power function ω^{-2n} , where the exponent depends on the symmetry of the electron state of the adsorbed atoms.¹⁵ When the contribution to the photoemission is made by resonant transitions from several surface levels or bands, the matrix T_a should be represented by a sum of several pole components.

It therefore follows that the matrix element M_1^s can be represented as follows:

$$M_1^s = c \frac{(\theta_a \Gamma)^{1/2}}{|\varepsilon_{eff}(x_1^0)|} \\ \times \left\{ \frac{E_0 - \hbar\omega}{\Gamma} \left[\arctan\left(-\frac{E_0 + \hbar\omega_0}{\Gamma}\right) - \arctan\left(-\frac{E_0 + \hbar\omega}{\Gamma}\right) \right] \right. \\ \left. + \frac{1}{2} \ln \left| \frac{(E_0 + \hbar\omega_0)^2 + \Gamma^2}{(E_0 + \hbar\omega)^2 + \Gamma^2} \right| \right\}^{1/2} \frac{1}{\omega^n}. \quad (14)$$

A calculation of the matrix element $|M_1^s|^2$ for the surface photoemission, involving variation of the parameters of the surface energy band $\rho_a(E)$ in a wide range of values, shows that the value of $|M_1^s|^2$ falls quite rapidly on increase in the photoexcitation frequency by an amount representing 2–3 eV from the photoemission threshold $\hbar\omega_0$. The value and the spectral dependence of the matrix element are influenced most by the position of the surface energy band near the Fermi level. The other parameters—the symmetry of the surface states n and the half-width Γ —have less influence on the nature of the matrix element.

In the calculation of the photoemission spectrum $I_p(\hbar\omega)$ we shall assume that $M_1 = M_1^s$, i.e., we shall ignore the bulk photoemission which is excited by the normal component of the electric field in the interior of the metal. As pointed out already, this is justified in the optical frequency range of the exciting light where $|\varepsilon_m| \gg 1$. The most suitable spectrum for the analysis of the parameters of the surface energy band is not simply $I_p(\hbar\omega)$, but a normalized spectrum $I_p(\hbar\omega)/I_s(\hbar\omega)$ [see Eqs. (5) and (7)]. In this case it is necessary to know the matrix elements $M_2^b(\hbar\omega)$ and $M_3^b(\hbar\omega)$. In the threshold frequency range in the case of metals we can assume, as established in many experiments that $M_2^b(\hbar\omega) = \text{const}$ and $M_3^b(\hbar\omega) = \text{const}$. We shall determine the ratio of the moduli and the difference between the phases of the matrix elements:

$$t = \left| \frac{M_1^s}{M_3^b} \right|, \quad \delta = \frac{1}{2} \ln \left| \frac{M_1^s}{M_3^b} \left(\frac{M_3^b}{M_1^s} \right)' \right|.$$

Figure 2 shows the spectra of I_p/I_s , calculated for the W(110)–Cs system with a monolayer whose coverage $\theta_a = 1$. Moreover, it is assumed that $\delta = 0.8$, $c|\varepsilon_{eff}(x_1^0)|^{-1} = 2$; $M_2^b = M_3^b = 1$; $t = 1$. The angle of incidence $\gamma = 45^\circ$ is the experimental value. Curves 1–6 in Fig. 2 demonstrate the evolution of this surface photoemission spectrum represented by I_p/I_s , when the band E_0 shifts near the Fermi level both in the direction of the empty states and also toward high binding energies. The energy position of the photoemission

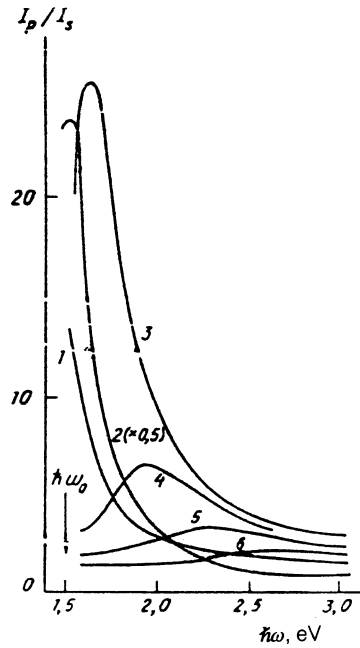


FIG. 2. Spectral dependence of I_p/I_s calculated for $\hbar\omega_0 = 1.50$ eV, $\Gamma = 0.05$ eV, $\varepsilon_m = 4.50 + 20.00i$, $\theta_a = 1$, $n = 2$, $\gamma = 45^\circ$, $t = 1$. The curves are plotted for the following values of E_0 (eV): 1) – 1.40; 2) – 1.50; 3) – 1.60; 4) – 1.80; 5) – 2.00; 6) – 2.50.

maximum of I_p/I_s is governed by the position of the energy band E_0 .

An analysis of the calculations carried out by varying other parameters (n and Γ) makes it possible to determine their influence on the nature of the spectrum of I_p/I_s . For example, the parameter n determines the slope of the short-wavelength edge of the spectrum, whereas Γ governs the half-width of the maximum of I_p/I_s . An allowance for the frequency dependence of the permittivity in the optical range ($\hbar\omega = 1\text{--}4$ eV) alters the ratio I_p/I_s by no more than 5%.

These calculations thus allow us to determine for the surface energy band that range of changes in its parameters which is most favorable for investigation in the threshold photoemission case: $E_F - 1.5$ eV $< E_0 \leq E_F$; $1 < n < 3.5$; $\Gamma \leq 0.3$ eV.

4. EXPERIMENTAL PHOTOEMISSION SPECTRA OF W(110)–Cs

We investigated for the first time ever the threshold photoemission spectra $I_s(\hbar\omega)$ and $I_p(\hbar\omega)$ when a submonolayer film of atomically pure Cs was deposited on the surface of tungsten. The coverage varied within the range $0.2 \leq \theta_a \leq 1.0$. The measurements were carried out in ultra-high vacuum ($P \leq 1 \times 10^{-10}$ Torr) at room temperature. Polarized monochromatic light ($\Delta\lambda = 40$ Å) was incident on the tungsten crystal at an angle $\gamma = 45^\circ$. The photoemission threshold $\hbar\omega_0$ was deduced from the spectrum $I_s(\hbar\omega)$ [see Eq. (5)].

In investigations of the angular dependences we used excitation with s and p -polarized light of the wavelength $\lambda = 6328$ Å. The method employed in recording the angular dependences (vector photoeffect) was described in Ref. 18.

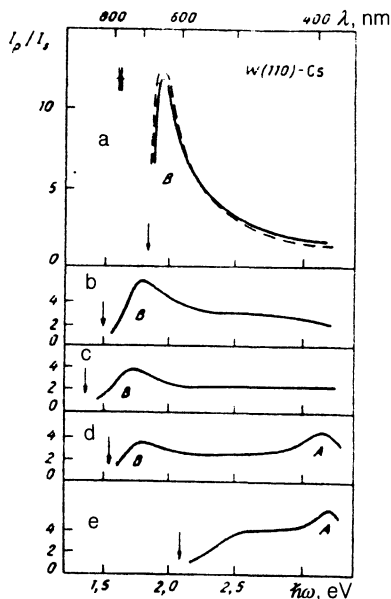


FIG. 3. Experimental spectra of the surface photoemission from the W(110)-Cs system obtained for different submonolayer coverages θ_a : a) $\theta_a = 0.95$ (the dashed curve is obtained by minimization of the parameters); b) 0.7; c) 0.6; d) 0.4; e) 0.3. The arrows identify the value of the photoemission threshold $\hbar\omega_0$.

Figure 3 shows the experimental photoemission spectra $I_p(\hbar\omega)/I_s(\hbar\omega)$ obtained for different values of θ_a . The arrows show the positions of the photoemission threshold $\hbar\omega_0$. The evolution of the spectrum demonstrates all the stages of the formation of the Cs energy band (maximum B) obtained in the range $\theta_a > 0.4$. The maximum A corresponds to the photoemission from the surface states of W(110). Its behavior on increase in θ_a is in good agreement with the data reported in Ref. 3.

An analysis of the experimental photoemission spectra represented by I_p/I_s was made in accordance with the above theoretical model taking an opportunity to reduce the number of independent parameters because they were determined from the angular photoemission dependences. Figure 4a gives the experimental curves $I_p(\gamma)$ obtained for different values θ_a of the Cs coating. Using Eqs. (5) and (7), knowing

the permittivity of tungsten $\epsilon(1.96 \text{ eV}) = 4.77 + 21.33i$ (Ref. 19) as well as the threshold $\hbar\omega_0$ for each coverage θ_a , we calculated the ratio of the moduli of the matrix elements $t^2 = |M_1^s|^2/M_3^b|^2$ from the angular dependences (Fig. 4b). It should be stressed that this value corresponded to a fixed excitation energy. A calculation was also made of the difference between the phases of the matrix elements, which was found to be constant: $\delta = 0.80 \pm 0.10$. The results obtained allowed us to determine for each θ_a the hitherto unknown coefficient $c|\epsilon_{\text{eff}}(x_1^0)|^{-1}$. The problem was therefore reduced to determination of three parameters of the surface energy band: E_0 , n , and Γ . These parameters were determined by minimization of the rms deviation between the experimental and theoretical curves, calculated from Eqs. (5) and (7), and allowing for Eq. (14). The error in this minimization procedure did not exceed 7% (dashed curve in Fig. 3).

Table I lists the parameters of the surface energy band, induced by the Cs coating, found by this method. It is worth noting that the formation of the surface energy band on increase in θ_a is accompanied by changes in all the fundamental parameters of the surface states.

5. CONCLUSIONS

The results reported above demonstrates that the threshold photoemission method can provide important information on the electron structure of adsorption layers on metal surfaces and this information cannot be obtained by the use of high-energy radiation. It must be stressed that in the optical frequency range the contribution of the microscopic surface region to the total photoemission signal can be separated because the effective field in the immediate vicinity of the interface is much stronger than the field in that part of the metal where the bulk photocurrent is formed. It is important to stress that the strong anisotropy of the properties of the investigated system means that the photoexcitation occurs mainly under the influence of the electric field component normal to the surface and this component varies rapidly near the interface. At higher frequencies, for example when synchrotron radiation is used, we have $|\epsilon_m| \approx 1$, so that the field in the region from which the bulk photocurrent

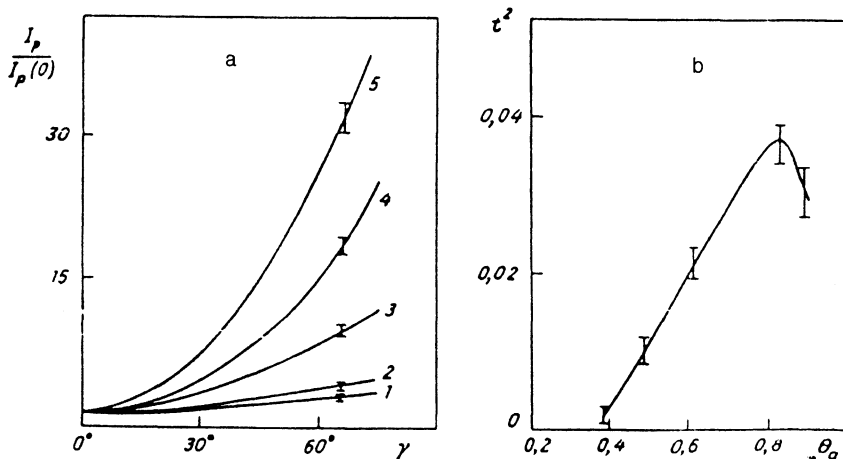


FIG. 4. a) Angular dependences of the photoemission current $I_p(\gamma)/I_p(0)$ obtained for the W(110)-Cs systems with different submonolayer coverages θ_a : 1) 0.60; 2) 0.45; 3) 0.77; 4) 0.85; 5) 1.00. b) Values of the ratio of the matrix elements t^2 , calculated at the frequency corresponding to $\hbar\omega = 1.96 \text{ eV}$ from the experimental angular dependences (Fig. 4a) of the W(110)-Cs system.

TABLE I. Parameters of the surface energy of the W(110)-Cs system with submonolayer coatings.

θ_a	$\hbar\omega_0$, eV	$E_F - E_0$, eV	n	Γ , eV
0.6	1.40±0.03	0.25±0.04	2.5±0.2	(0.8±0.4) · 10 ⁻²
0.7	1.44±0.03	0.18±0.04	2.2±0.2	(2.0±0.7) · 10 ⁻²
0.8	1.62±0.03	0.12±0.03	1.8±0.2	(3.5±0.9) · 10 ⁻²
0.9	1.78±0.03	0.08±0.03	1.5±0.2	(5.0±1.5) · 10 ⁻²
1.0	1.94±0.03	0.06±0.03	1.1±0.2	(6±2) · 10 ⁻²

is obtained is approximately equal to the field in the adsorption layer. The contribution of the adsorbate is then small compared with the bulk photocurrent. The role of the microscopic region near the interface becomes greater in the presence of alkali adsorbates on the tungsten surface, because their influence gives rise to a boundary region with a lower effective permittivity and, consequently, it enhances additionally the intensity of the field at the surface. A quantum-mechanical calculation of the influence of the alkali adsorbates on the behavior of $\epsilon_{\text{eff}}(x_1)$ carried out using the "jellium" model can be found in Ref. 14.

An analysis of the experimental photoemission spectra by means of Eqs. (7) and (13) allowed us to determine the position and half-width of the surface energy band induced by adsorption, as well as the dependences of these two parameters on the coverage. A reliable determination of these parameters required the use also of the experimental angular and polarization dependences of the photoemission process, which—as demonstrated above—were described well by Eqs. (5) and (7). It should be stressed that our angular dependences of the photoemission current induced by *p*-polarized light were not correlated with the dependence of the absorbed power of the optical wave on the angle γ , as postulated earlier in numerous investigations of the photoeffect.^{20,21} In particular, the absorbed power hardly changes due to the appearance of an adsorbate, whereas the experimentally determined dependence $I_p(\gamma)/I_p(0)$ exhibits qualitative changes when the coverage θ_a is varied.

¹S. Lundqvist and N. H. March (eds.), *Theory of Inhomogeneous Electron Gas*, Plenum Press, New York (1983).

²S. -L. Weng, J. I. Inglesfeld, D. A. King, and C. Somerton, *J. Phys. C* **14**, 309 (1981).

³P. Soukiasian, R. Riwan, J. Lecante, E. Wimmer *et al.*, *Phys. Rev. B* **31**, 4911 (1985).

⁴G. V. Hansson and S. A. Flodström, *Phys. Rev. B* **18**, 1562 (1978).

⁵S. D. Kevan and R. H. Gaylord, *Phys. Rev. B* **36**, 5809 (1987).

⁶G. V. Benemanskaya and M. N. Lapushkin, *Pis'ma Zh. Eksp. Teor. Fiz.* **45**, 423 (1987) [*JETP Lett.* **45**, 540 (1987)].

⁷S. A. Lindgren and L. Wallden, *Solid State Commun.* **28**, 283 (1978).

⁸S. A. Lindgren and L. Wallden, *Solid State Commun.* **34**, 671 (1980).

⁹G. V. Benemanskaya and M. N. Lapushkin, *Pis'ma Zh. Eksp. Teor. Fiz.* **41**, 432 (1985) [*JETP Lett.* **41**, 531 (1985)].

¹⁰K. Horn, A. Hohlfeld, J. Somers *et al.*, *Phys. Rev. Lett.* **61**, 2488 (1988).

¹¹K. -H. Frank, H. -J. Sagner, and D. Heskett, *Phys. Rev. B* **40**, 2767 (1989).

¹²G. V. Benemanskaya, G. P. Burmistrova, and M. N. Lapushkin, *Phys. Lett. A* **137**, 139 (1989).

¹³A. M. Brodsky and M. I. Urbakh, *Prog. Surf. Sci.* **15**, 121 (1984).

¹⁴A. Liebsch, *Phys. Rev. B* **40**, 3421 (1989).

¹⁵A. M. Brodskii and M. I. Urbakh, *Electrodynamics of the Metal / Electrolyte Interface*, Nauka, Moscow (1989).

¹⁶A. Bagchi and N. Kar, *Phys. Rev. B* **18**, 5240 (1978).

¹⁷J. R. Smith (ed.), *Theory of Chemisorption*, Springer Verlag, Berlin (1980) [*Topics in Current Physics*, Vol. 19].

¹⁸G. V. Benemanskaya and M. N. Lapushkin, *Pis'ma Zh. Eksp. Teor. Fiz.* **49**, 515 (1989) [*JETP Lett.* **49**, 595 (1989)].

¹⁹J. H. Weaver, C. G. Olson, and D. W. Lynch, *Phys. Rev. B* **12**, 1293 (1975).

²⁰D. W. Juenker, J. P. Waldron, and R. J. Jaccodine, *J. Opt. Soc. Am.* **54**, 216 (1964).

²¹P. O. Gartland, S. Berge, and B. J. Slagsvold, *Phys. Rev. Lett.* **30**, 916 (1973).

Translated by A. Tybulewicz